

# Griffiths effects and quantum critical points in dirty superconductors without spin-rotation invariance: One-dimensional examples

Olexei Motrunich,<sup>1</sup> Kedar Damle,<sup>1,2</sup> and David A. Huse<sup>1</sup>

<sup>1</sup> *Physics Department, Princeton University, Princeton, NJ 08544*

<sup>2</sup> *Physics Department, Harvard University, Cambridge, MA 02138*

(November 10, 2000)

We introduce a strong-disorder renormalization group (RG) approach suitable for investigating the quasiparticle excitations of disordered superconductors in which the quasiparticle spin is not conserved. We analyze one-dimensional models with this RG and with elementary transfer matrix methods. We find that such models with broken spin rotation invariance *generically* lie in one of two topologically distinct localized phases. Close enough to the critical point separating the two phases, the system has a power-law divergent low-energy density of states (with a non-universal continuously varying power-law) in either phase, due to quantum Griffiths singularities. This critical point belongs to the same infinite-disorder universality class as the one dimensional particle-hole symmetric Anderson localization problem, while the Griffiths phases in the vicinity of the transition are controlled by lines of strong (but not infinite) disorder fixed points terminating in the critical point.

## I. INTRODUCTION

Recently, there has been considerable theoretical activity concerning the effect of disorder on the quasiparticle spectrum in dirty superconductors with different pairing symmetries.<sup>1,2</sup> The basic philosophy underlying most of these developments is to start with a weakly disordered problem and investigate the fate (in some RG sense) of disorder at large length scales using field theoretic methods.<sup>3</sup> An analysis of this sort depends most crucially on the possible symmetries of the quasiparticle Hamiltonian, and it is the corresponding universal properties that have received most attention thus far. These include the leading effects of disorder on the conductivity and density of states in the delocalized regime, as well as the universal scaling properties of the localization transition.

Our focus in this article is quite different: We ask if Griffiths effects, whereby rare configurations of the disorder potential over large regions of space give rise to *non-universal* contributions that dominate some low-energy property, may be important in dirty superconductors. In particular, are there situations in which such Griffiths effects lead to a singular enhancement in the quasiparticle density of states near the Fermi energy? Unfortunately, this intriguing possibility has not attracted much attention in previous work.

Such issues are difficult to address within the weak-disorder framework mentioned above. Instead, we introduce a RG approach that is suitable for situations in which the effective value of disorder becomes large at low energies. Our basic result is simply stated: It is indeed possible for such Griffiths effects to dominate the low-energy properties, at least in one-dimensional models with either triplet pairing, or strong spin-orbit effects, or spin-flip scattering off frozen magnetic impurities. More specifically, we show that such models with broken spin rotation (SR) invariance *generically* lie in one of two

distinct localized phases. These two phases are distinguished by a topological property (reflected in the presence or absence of zero-energy end-states in a large but finite wire) that makes it impossible to go smoothly from one phase to the other. At the phase transition separating the two, the effective disorder grows without bound when viewed on ever-smaller energy scales, and the low-energy density of states behaves as  $\rho(\epsilon) \sim 1/|\ln^3 \epsilon|$  (Dyson<sup>4</sup> singularity). The localized phases near this transition, on both sides, are *Griffiths phases* having a power-law singularity (with a non-universal exponent) in the low-energy density of states; these Griffiths phases are themselves characterized by strong (but not infinite) effective disorder in the limit of low energies. [Note that a recent weak-disorder analysis, Refs. 5 and 6, of this problem has been carried out only at criticality. The results of Refs. 5,6 for the thermal conductance and the density of states are consistent with the predictions of our RG approach at such a critical point—however, as we show here, the generic behavior of the system is localized rather than critical.<sup>7</sup>]

The detailed scaling properties of the low-energy strong-disorder critical point and the nearby Griffiths phases are, of course, specific to our one-dimensional examples. However, our RG approach is well suited for studying possible Griffiths effects in two or more dimensions as well, and some speculations along these lines are briefly discussed towards the end of this article.

## II. PHYSICAL PICTURE AND MOTIVATION

Before plunging into the details of our analysis, it is useful to have a heuristic picture of the basic physics of our 1d problems. To this end, we consider a simple toy model for a disordered *spinless* (more physically, *spin-polarized triplet*) superconducting ‘wire’ with a sin-

gle transverse mode (channel) active. We model our system by a lattice Bogoliubov-de Gennes (BdG) Hamiltonian

$$\hat{H} = \sum_n (tc_n^\dagger c_{n+1} + \Delta c_n^\dagger c_{n+1}^\dagger + \text{h.c.}) + \sum_n \epsilon_n c_n^\dagger c_n. \quad (1)$$

In this toy model, the nearest neighbor hopping amplitude  $t$  and the “p-wave” pairing amplitude  $\Delta$  are real constants, while the impurity potential  $\epsilon_n$  can take on values  $V_1$  and  $V_2$  with some probabilities  $p$  and  $1 - p$  respectively. Furthermore, we stipulate that  $|V_1| < V_c$  and  $|V_2| > V_c$ , where  $V_c \equiv 2|t|$ .

The significance of the critical value  $V_c$  is readily seen by solving the pure problem with fixed  $\epsilon_n = V$ , i.e., with the chemical potential equal to  $-V$ . One easily finds that there is a gap in the quasiparticle excitation spectrum around the Fermi energy for both  $|V| > V_c$  and  $|V| < V_c$ . However, at the critical point  $|V| = V_c$ , the system is gapless. Thus, there are two different gapped phases for our pure system (the phase with  $|V| > V_c$  simply corresponds, in the absence of the pairing term, to a situation in which the Fermi level has gone below the bottom of the band or above the top of the band; thus, it is essentially a ‘band insulator’). For our purposes here, the important distinction between the two phases has to do with low-energy bound states at the ends of a long but finite wire of length  $L$  with free boundary conditions. In the ‘gapped superconductor’ phase with  $|V| < V_c$ , such a wire has a single quasiparticle state below the gap with an excitation energy that is exponentially small in the length  $L$ ; the corresponding wavefunction has weight only in the vicinity of the two ends of the chain (in the language of Ref. 8, in the  $L \rightarrow \infty$  limit, we thus have two zero-energy Majorana fermions, one at each end of the chain). In the other gapped phase,  $|V| > V_c$ , there is no such low-energy quasiparticle state.<sup>9</sup>

Now, imagine a disorder realization in which the potential has value  $V_1$  throughout the region between, say, sites 0 and  $L$ , and value  $V_2$  out to a distance  $L$  on either side of this central segment. The value of the potential is left unspecified in the rest of the system. The probability of this happening is  $p^L(1 - p)^{2L} = e^{-cL}$ , with  $c$  appropriately defined. Now, the central region can be thought of, for large  $L$ , as a finite wire in the phase with  $|V| < V_c$  surrounded by *vacuum* (this is reasonable since the long segments on either side can be roughly thought of as regions with no particle because the Fermi energy  $-V_2$  has gone below the bottom of the band; effective couplings of the central region with the rest of the system, mediated through such isolating segments, are exponentially small in  $L$ ). Such a situation will lead to a low-energy quasiparticle state with excitation energy  $\epsilon_L \sim e^{-c'L}$ , with some  $c'$  of order one. Since such low-energy states living on ‘domain walls’ between large regions in ‘opposite’ phases can happen anywhere along the entire length of our wire, such disorder configurations will give a non-zero contribution in the thermodynamic limit to the density of states. This contribution can be estimated as

$\rho_{\text{Griff}}(\epsilon) = \int dL \delta(\epsilon - e^{-c'L})e^{-cL} \sim \epsilon^{-1+1/z}$ , where we have introduced the dynamical exponent  $z = c'/c$ . This serves as a lower bound on the actual low-energy density of states in our disordered problem—thus, we *generically* have a power-law behavior (with a non-universal continuously varying exponent) of the density of low-energy excitations in our toy model. Although this model is admittedly crude, the picture of rare configurations of disorder over large regions of space leading to singular low-energy behavior is at the heart of the more precise strong-disorder RG analysis of Section VI.

We conclude this section with some comments on our choice of toy-model, and, more generally, on the results obtained in this article. Firstly, note that we completely ignored the self-consistency condition that, in principle, determines  $\Delta$  in terms of the other parameters.<sup>10,11</sup> This is not expected to matter; in fact, the precise choices made for various parameter values are not very important for our conclusion—nor is it important that our toy-model has time reversal symmetry. As far as this model is concerned, the only important thing is the existence of two different gapped phases, with one of them supporting zero-energy end-states. [Note that this is the main distinction of our models without SR-invariance from the models with SR-invariance: When the quasiparticle spin is a good quantum number, there are no such end-states in any finite open chain, and we expect no Griffiths effects in this case—this will also become clear from our more detailed RG analysis.]

Another concern is that we are treating a one-dimensional superconductor with the BdG equations, which ignore quantum fluctuations of the condensate order parameter  $\Delta$ . When the superconductor is in more than one dimension,  $\Delta$  does have a nonvanishing static component at zero temperature, but in a strictly one-dimensional system, divergent quantum fluctuations mean that the superconducting state does not have true long range order or a gap. However, in highly anisotropic quasi-one-dimensional superconductors,  $T_c$  (and the gap) can, in principle, be large compared to the interchain hopping energy, and our approach should then apply in the range between these two energy scales (while no such regime appears to exist in quasi-one-dimensional superconductors known so far, *a priori*, there are no physical reasons that would prevent this from happening in some cases<sup>12</sup>). Another possible physical realization<sup>1</sup> is that of a vortex in a three dimensional gapped superconductor in the presence of frozen magnetic impurities or spin-orbit scattering. In such a situation, the effect of disorder on the quasiparticle states confined to the vortex core can be analyzed by a 1d BdG equation approach such as the one we employ. Naturally, the choice of probability distributions for various quenched random variables will be different depending on the physical realization one is interested in (for instance, it is more natural to use a quenched random  $\Delta$  with zero mean when considering the vortex problem). However, as will be clear from our later analysis, the precise form of the probability distri-

bution for various bare couplings in the problem does not play an important role in determining the nature of the low-energy physics.

Finally, note that the effects of the residual quasiparticle interactions are beyond the scope of our analysis.

### III. FORMALISM, SYMMETRY CLASSES, AND OUR 1D MODELS

It is useful to set up notation and review some basics<sup>13,2</sup> before proceeding to our actual calculations. To this end, consider a general lattice BdG Hamiltonian

$$\hat{H}_{SC} = \sum_{\alpha\beta} \left( h_{\alpha\beta} c_{\alpha}^{\dagger} c_{\beta} + \frac{1}{2} \Delta_{\alpha\beta} c_{\alpha}^{\dagger} c_{\beta}^{\dagger} + \frac{1}{2} \Delta_{\alpha\beta}^{*} c_{\beta} c_{\alpha} \right), \quad (2)$$

where we use a composite label  $\alpha = \{i, \mu\}$  for the site and spin indices of fermion orbitals. Hopping amplitudes, the effects of spin-orbit interaction on the hopping amplitudes, spin-flip scattering from frozen magnetic impurities, and random potential terms corresponding to non-magnetic impurities are now all included in  $h_{i\mu, j\nu}$ , while pairing amplitudes are represented by  $\Delta_{i\mu, j\nu}$ . Hermiticity requires  $h_{\beta\alpha} = h_{\alpha\beta}^{*}$ , and we choose  $\Delta_{\beta\alpha} = -\Delta_{\alpha\beta}$  consistent with the fermion anticommutation relations. Additional restrictions (to be reviewed below) arise when T-invariance is a good symmetry (we will *not* consider cases with SR-invariance in this article).

The spectrum of quasiparticle excitations for  $\hat{H}_{SC}$  is specified by the spectrum of a (Hermitian) matrix

$$\mathcal{H} = \begin{pmatrix} h & \Delta \\ -\Delta^{*} & -h^{*} \end{pmatrix} \quad (3)$$

acting in an enlarged “particle-hole” Hilbert space. A particle/hole mixing unitary transformation  $U_0 = \frac{1}{\sqrt{2}} \begin{pmatrix} 1 & -i \\ 1 & i \end{pmatrix} \otimes \mathbf{1}_{2N}$  (where  $N$  is the number of lattice sites), which acts independently on states corresponding to each  $\alpha$ , transforms  $\mathcal{H}$  into an antisymmetric *pure imaginary* form

$$\mathcal{H}_{Im} = U_0^{-1} \mathcal{H} U_0 = \begin{pmatrix} i \operatorname{Im}(h + \Delta) & i \operatorname{Re}(-h + \Delta) \\ i \operatorname{Re}(h + \Delta) & i \operatorname{Im}(h - \Delta) \end{pmatrix}. \quad (4)$$

This representation is well-suited for a discussion of heat transport properties of the quasiparticles. Indeed, the quasiparticle thermal conductivity is simply proportional to  $k_B T \sigma$ , where  $\sigma$  is the  $T = 0$  conductivity of a (normal) system of non-interacting fermions described by the lattice Schroedinger equation corresponding to  $\mathcal{H}_{Im}$  (see Ref. 2 and references therein). [Note that  $\mathcal{H}_{Im}$  may also be obtained, as in Ref. 2, from the original  $\hat{H}_{SC}$  by writing everything in terms of Majorana fermions and then doubling the system, and we will therefore use a “copy index”  $K$  below to label the different blocks of  $\mathcal{H}_{Im}$ .]

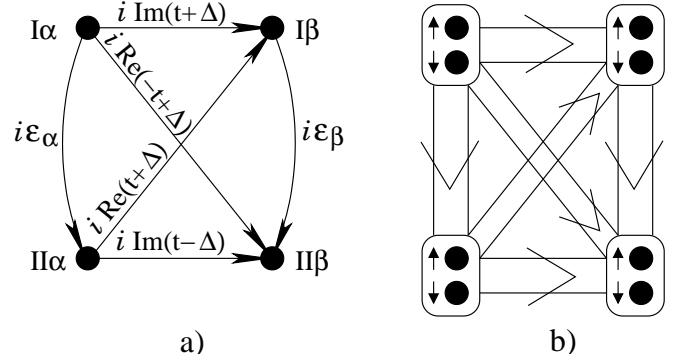


FIG. 1. a) General pure imaginary representation of hopping ( $t$ ) and pairing ( $\Delta$ ) couplings between two fermion orbitals  $\alpha$  and  $\beta$ ; b) in the T-invariant case, it is more convenient (see text) to work with block-sites and block-couplings shown here.

Most of our discussion will use this pure imaginary form. In the absence of both SR-invariance and T-invariance, the different matrix elements of  $\mathcal{H}_{Im}$  take on roughly independent imaginary values (apart from the requirements imposed by hermiticity). Thus, we have a general *pure imaginary* random hopping (ImRH) problem on a *doubled* lattice. Each original fermion orbital  $\alpha = \{i, \mu\}$  is “represented” by two “copies”  $I\alpha$  and  $II\alpha$ ; the energy of an orbital  $\alpha$  is represented by an imaginary hopping amplitude between  $I\alpha$  and  $II\alpha$ , while hopping and pairing amplitudes between two orbitals  $\alpha$  and  $\beta$  are represented by imaginary hopping amplitudes between the two pairs  $\{I\alpha, II\alpha\}$  and  $\{I\beta, II\beta\}$  (see Fig. 1a).

In the presence of T-invariance,  $h$  and  $\Delta$  satisfy  $\sigma_y h^* \sigma_y = h$  and  $\sigma_y \Delta^* \sigma_y = \Delta$ , where  $\sigma_y = \sigma_y \otimes \mathbf{1}_N$  and  $\sigma_y$  acts on the spin degree of freedom at each site. The corresponding restrictions on  $\mathcal{H}_{Im}$  are best stated as follows: Group the different spin states on the same lattice site  $i$  and with the same copy index  $K$  into a block pair  $\{Ki \uparrow, Ki \downarrow\}$ . T-invariance then implies that there are no internal couplings within such blocks. Moreover, the couplings between two blocks with the same copy index have a form

$$\hat{t}_{\text{block}} = \begin{pmatrix} i a & i b \\ i b & -i a \end{pmatrix} = i r \begin{pmatrix} \cos \theta & \sin \theta \\ \sin \theta & -\cos \theta \end{pmatrix} \quad (5)$$

with real  $a$  and  $b$  ( $r = \sqrt{a^2 + b^2}$ ), while the couplings between two blocks with different copy indices have a form  $\begin{pmatrix} i c & -i d \\ i d & i c \end{pmatrix}$  with real  $c$  and  $d$ . Simply relabeling the spin states of copy II brings all block-couplings to the same form Eq. (5), and we will find it convenient to discuss the T-invariant case using this picture of block-sites connected by block-couplings (see Fig. 1b where each fat arrow represents the corresponding block coupling Eq. (5) with independent  $a$  and  $b$ , and different arrows are roughly independent of each other). We also use another representation of  $\mathcal{H}$  in the T-invariant

case: This is obtained<sup>13</sup> by performing a particle/hole and spin-up/down mixing unitary transformation  $U_\tau = \frac{1}{\sqrt{2}}(\mathbf{1}_2 \otimes \tau_z + \sigma_y \otimes \tau_x) \otimes \mathbf{1}_N$  (here,  $\mathbf{1}_2$  and the Pauli matrix  $\sigma_y$  act on the spin label, while the Pauli matrices  $\tau$  act on the particle-hole label):

$$\mathcal{H}_\tau = U_\tau^{-1} \mathcal{H} U_\tau = \begin{pmatrix} 0 & h\sigma_y - \Delta \\ \sigma_y h + \Delta^* & 0 \end{pmatrix}. \quad (6)$$

$\mathcal{H}_\tau$  thus has a *bipartite* complex hopping form, which will prove useful for our transfer matrix analysis (note however that strong correlations among matrix elements of  $\mathcal{H}_\tau$  limit its usefulness in other contexts).

Finally, in the spinless case with no T-invariance, we simply drop the spin label altogether and do not have any constraints on the bonds of the corresponding ImRH problem. [Here and elsewhere in this article, we use the designation ‘spinless’ to also refer to all situations in which the spin label of the electron can be dropped—such as spin-polarized triplet superconductors. Also, in the rest of this article, we do not consider specifically the spinless case with T-invariance, but only mention the relevant results as we go along. This case is very special<sup>2</sup> and maps onto a class of bipartite hopping problems that have been studied both in one<sup>14</sup> and two<sup>15</sup> dimensions. In one dimension, our RG approach yields results consistent with what is known from Ref. 14 and can provide more details about the low-energy properties of any particular system in this universality class, while some two-dimensional systems in this universality class will be discussed separately.<sup>16]</sup>

In this paper, we consider three one-dimensional systems: the spinless superconductor without T-invariance, the ‘spinful’ T-invariant superconductor, and the ‘spinful’ superconductor without T-invariance. In all three examples, the bulk of our discussion is for the case with a single transverse mode (channel) present. However, as will become clear from our analysis of the ‘spinful’ superconductor without T-invariance, our basic conclusions regarding the low-energy physics *apply equally well for the multi-channel case of all three problems*.

We model these systems by the appropriate BdG Hamiltonians with only nearest neighbor hopping and pairing amplitudes, in addition to same-lattice-site terms (the restriction to such nearest neighbor models is not at all crucial for any of our conclusions). The ImRH problem corresponding to the single-channel spinless case is a two-leg ladder with all couplings pure-imaginary and roughly independent, but no other restrictions—in particular, couplings along the rungs of the ladder are allowed. Such ‘rung-couplings’ (which we will sometimes refer to as ‘vertical’ couplings—see Fig. 1a) correspond to any on-site terms in the original lattice BdG Hamiltonian; in the spinless case, these can only be random potential terms, but more generally, one can also have “s-wave” pairing amplitudes and spin-flip scattering potentials (the latter due to frozen magnetic impurities).

For the single-channel ‘spinful’ T-invariant case, the corresponding ImRH problem is an analogous two-leg ladder of block-sites with pure imaginary block-couplings that are roughly independent of one another—in other words, we have a four-leg ladder with this special block structure. Finally, the single-channel ‘spinful’ case without T-invariance is a pure-imaginary four-leg ladder with no other restrictions. These ladder problems are related to the bipartite random hopping (RH) ladder problems<sup>14</sup> in which rung couplings are disallowed but the other hopping amplitudes do not have to be pure imaginary—as mentioned earlier, these are in the same universality class as spinless superconducting wires with T-invariance. [The connection between this special class of models with sublattice symmetry and the more general systems that we study here is in fact surprisingly close, as will become apparent from our transfer matrix and RG analyses.]

Finally, it is worth emphasizing at this point that our focus in all these cases is on the low-energy physics: The systems mentioned above will all differ from each other at higher energy scales, particularly in the initial ‘diffusive’ crossover regime that would be present in any weakly-disordered problem. However, at energies below this crossover scale, the effective value of disorder becomes large and all these systems can be described by a unified physical picture.

#### IV. STRONG-RANDOMNESS RG APPROACH

In order to go beyond the heuristic ideas of Sec. II, we need a *controlled* approach that works in situations with strong Griffiths effects (such that  $z$ , defined by the low-energy behavior  $\rho(\epsilon) \sim \epsilon^{-1+1/z}$  of the density of states, is large). Such situations are expected to correspond to large values of effective disorder in the low-energy limit (in fact, a simple scaling argument indicates that the width of the distribution of the logarithms of the effective couplings is expected to be of order  $z$  in the low-energy limit). We are thus led to formulate a strong-disorder RG approach to this problem.

Consider the ImRH Hamiltonian  $\mathcal{H}_{\text{Im}} = \sum_{ij} t_{ij} |i\rangle\langle j|$  with  $t_{ji} = t_{ij}^* = -t_{ij}$ . The eigenstates of  $\mathcal{H}_{\text{Im}}$  occur in pairs with energies  $\pm\epsilon$ , and the strong-randomness RG proceeds by eliminating, at each step, such a pair of states with energies at the top and at the bottom of the band: One finds the largest (in absolute value) coupling in the system, say  $t_{12}$  connecting sites 1 and 2; this defines the bandwidth of the problem  $2\Omega = 2\max\{|t_{ij}|\}$ . If the distribution of the couplings is broad, the eigenfunctions of the two-site problem  $\mathcal{H}_{\text{Im}}[1, 2]$  will be good approximations to the eigenstates with energies  $\pm\Omega$ , since the couplings  $t_{1j}$  and  $t_{2j}$  of the pair to the rest of the system will typically be much smaller. These couplings can then be treated perturbatively, and eliminating the high-energy states living on the sites 1 and 2 gives us the following effective couplings between the remaining sites:

$$\tilde{t}_{ij} = t_{ij} - t_{i1}(t_{12}^\dagger)^{-1}t_{2j} - t_{i2}(t_{21}^\dagger)^{-1}t_{1j}. \quad (7)$$

Clearly, the renormalized Hamiltonian  $\tilde{\mathcal{H}}_{\text{Im}}$  again corresponds to a pure imaginary hopping problem, but with two fewer sites; in particular, the matrix  $\tilde{\mathcal{H}}_{\text{Im}}$  has no diagonal terms,<sup>18</sup>  $\tilde{t}_{ii} \equiv 0$ .

Some remarks on the proposed RG approach are in order here. Note that our RG rule Eq. (7) is an *exact* transformation for the zero-energy wavefunction, and as such provides information on the zero-energy localization properties. From a numerical point of view, it can be viewed as a construction of the zero-energy wavefunction in an *a priori* stable manner. Moreover, this transformation can also be viewed as an approximate but accurate scheme for evaluating the ‘Sturm sequence’, i.e., the integrated density at very low energies, with the approximations involved being well-controlled when the low-energy effective couplings are broadly distributed. Lastly, note that in the limit of strong disorder and in the absence of strong correlations between different couplings, the right hand-side of Eq. (7) can be replaced with the “max” (in absolute value) of the three terms.

So far, we have ignored the restrictions that would be imposed on the couplings of the ImRH problem in a ‘spinful’ (i.e., when both spin species need to be considered) T-invariant situation. In this case, it is more natural to work with the block-sites and block-couplings defined earlier (Fig. 1b). To begin with, note that the eigenstates now occur in *doubly degenerate* pairs with energies  $\pm\epsilon$ . Thinking in terms of blocks automatically incorporates this degeneracy, since the eigenstates of a two-block-site problem  $\mathcal{H}_\tau[1, 2]$  come in such doubly degenerate pairs with energies  $\pm r_{12} = \pm\sqrt{a_{12}^2 + b_{12}^2}$ . Our RG approach now eliminates four states at each step, two at the top and two at the bottom of the band with energies  $\pm\Omega$ , where  $\Omega \equiv \max\{r_{ij}\}$ . The resulting effective block-couplings among the remaining block-sites are again given by Eq. (7), but now each  $\hat{t}_{ij}$  is a  $2 \times 2$  matrix of the form (5). The effective problem is again an ImRH problem in the same block-form, and no block-diagonal terms are generated. For the RG rule Eq. (7), the flows of bond-energies  $r$  and bond-angles  $\theta$  do not separate. However, for strong disorder and in the absence of strong correlations (i.e., roughly, when the “max” RG rule applies) the energy variables  $r$  flow exactly as in the ImRH representation of a spinless superconductor without T-invariance, while the angle variables simply randomize. Thus, we expect essentially identical results for this ‘spinful’ problem with T-invariance and the corresponding spinless problem without T-invariance *when both flow to strong disorder sufficiently rapidly*.

## V. CRITICAL POINTS AND GRIFFITHS EFFECTS IN 1D: TRANSFER MATRIX ANALYSIS

Before we go on to our more detailed RG analysis of the low-energy properties, it is useful to have a picture of the phase diagram in each case. We use an elementary transfer matrix analysis to develop such a picture in terms of the zero-energy localization properties of the system. The goal here is to show by direct means that *generically* all our models are localized, and to demonstrate that there are critical points representing transitions between distinct localized phases; of course, these critical points can only be accessed by fine-tuning the disorder distributions.

In general terms, we are looking at the zero-energy localization properties of  $M$ -leg ladder systems governed by a Schroedinger equation

$$\epsilon\vec{\psi}_n = \hat{t}_n\vec{\psi}_{n+1} + \hat{t}_{n-1}^\dagger\vec{\psi}_{n-1} + \hat{u}_n\vec{\psi}_n, \quad (8)$$

where  $\hat{t}_n$  and  $\hat{u}_n$  are  $M \times M$  matrices, and the wavefunction  $\vec{\psi}_n$  is an  $M$ -dimensional vector defined at each rung  $n$ . We find it convenient to work with the following transfer matrix formulation:

$$\begin{pmatrix} \vec{\psi}_{n+1} \\ \hat{t}_n^\dagger\vec{\psi}_n \end{pmatrix} = \begin{pmatrix} \hat{t}_n^{-1}(\epsilon - \hat{u}_n) & -\hat{t}_n^{-1} \\ \hat{t}_n^\dagger & 0 \end{pmatrix} \begin{pmatrix} \vec{\psi}_n \\ \hat{t}_{n-1}^\dagger\vec{\psi}_{n-1} \end{pmatrix}; \quad (9)$$

this defines elementary transfer matrix  $\hat{T}_n$ .

### 1. The bi-partite ladder problems:

To begin with, consider the bipartite problem mentioned above, in which one has  $M$  coupled chains with no rung couplings,  $\hat{u}_n \equiv 0$ . This system was studied by Brouwer *et. al.*,<sup>14</sup> who found that for both real or complex hopping amplitudes there are  $M+1$  localized phases separated by  $M$  dimerization driven delocalized critical points; each critical point exhibits a strong Dyson singularity in the density of states,  $\rho(\epsilon) \sim 1/|\ln^3 \epsilon|$ . Here, we rederive by completely elementary means the existence of  $M$  delocalized critical points, and also characterize the  $M+1$  distinct localized phases; the ideas introduced in the process will generalize naturally to our superconductor systems.

Being bipartite, the two sublattices decouple at  $\epsilon = 0$ :

$$\hat{T}_{n+1}\hat{T}_n = \begin{pmatrix} -\hat{t}_{n+1}^{-1}\hat{t}_n^\dagger & 0 \\ 0 & -\hat{t}_{n+1}^\dagger\hat{t}_n^{-1} \end{pmatrix}. \quad (10)$$

We are thus led to study the Lyapunov spectrum of the matrix products  $\hat{t}_{2k}^{-1}\hat{t}_{2k-1}^\dagger \dots \hat{t}_2^{-1}\hat{t}_1^\dagger$  and  $\hat{t}_{2k}^\dagger\hat{t}_{2k-1}^{-1} \dots \hat{t}_2^\dagger\hat{t}_1^{-1}$ . At zero dimerization ( $\hat{t}_{2k}$  and  $\hat{t}_{2k+1}$  distributed identically) the Lyapunov spectra of both products (consisting of  $M$  distinct Lyapunov exponents in the general case) are identical and symmetric around zero, and the full

Lyapunov spectrum (of the full transfer matrix product) is doubly degenerate. Thus, for even  $M$  the smallest (in absolute value) Lyapunov exponent is non-zero and the zero-energy modes are localized, while for odd  $M$  there is always a zero Lyapunov exponent. [The actual values of these exponents are not of much concern here, only the fact that they are all distinct.] Now, consider adding dimerization by simply multiplying every odd bond  $\hat{t}_{2k+1}$  by a scale factor  $e^\delta$  and every even bond  $\hat{t}_{2k}$  by a factor  $e^{-\delta}$ . Clearly, the whole Lyapunov spectrum for one reduced (sublattice) problem is shifted rigidly by  $\delta$  (and by the exactly opposite amount for the other sublattice). Thus, as we scan  $\delta$  from  $-\infty$  to  $+\infty$ , there will be exactly  $M$  points where two of these exponents of the full transfer matrix cross zero. For the given sublattice, if we label each non-critical region by  $(k, M-k)$  with  $k$  growing modes and  $M-k$  decaying modes, these critical points represent consecutive “delocalization” transitions  $(k, M-k) \rightarrow (k+1, M-k-1)$ . Of course, this can also be restated in terms of the number of zero-energy states localized at each end in a finite odd-length chain with free boundary conditions, and provides a ‘topological’ distinction between the different localized phases; each transition corresponds to a single zero-energy state becoming delocalized and migrating from one end of the chain to the other.

In a bulk system, at any of these critical points, one has two zero-energy delocalized *Lyapunov modes* (linear combinations of which can roughly be interpreted as a ‘left-moving’ and a ‘right-moving’ slow modes). Since any description of the low-energy properties of the critical system in terms of such ‘slow’ modes has to respect the bipartite nature of the original problem, it is natural to expect that such a low-energy effective theory is in the same universality class as the bipartite single chain RH problem.<sup>19</sup> This provides a clear rationale for the critical low-energy density of states to be of the Dyson form. Similarly, we expect that the localized phases in the vicinity of any critical point look, at low energies, like the dimerized Griffiths phases obtained by introducing a small amount of dimerization in the single chain problem—in particular, we expect Griffiths singularities in the density of states consistent with the results of Ref. 14.

## 2. Single-channel spinless superconductor without $T$ -invariance:

Returning to the dirty superconductor problems, consider first the spinless fermion system with no  $T$ -invariance in the ImRH language. In this case, the rung coupling is of the form  $\hat{u}_n = \mu_n \sigma_y$  with some real  $\mu_n$  ( $\sigma_y$  acts on the copy label  $K$ ), while the hopping term is a general pure imaginary  $2 \times 2$  matrix  $\hat{t}_n$ . Because of the identity  $\sigma_y \hat{a}^{-1} \sigma_y = \hat{a}^T / \det \hat{a}$  valid for any  $2 \times 2$  matrix  $\hat{a}$ , the zero-energy transfer matrices “decouple”:

$$\hat{T}_n = - \begin{pmatrix} 1 & 0 \\ 0 & \sigma_y \end{pmatrix} \begin{pmatrix} \mu_n \hat{t}_n^{-1} \sigma_y & \hat{t}_n^{-1} \sigma_y \\ \tau_n \hat{t}_n^{-1} \sigma_y & 0 \end{pmatrix} \begin{pmatrix} 1 & 0 \\ 0 & \sigma_y \end{pmatrix}, \quad (11)$$

where  $\tau_n = \det \hat{t}_n$ . Thus, Lyapunov exponents of the product of  $\hat{T}_n$  are given by a “superposition” of the Lyapunov exponents of the product of  $\sqrt{|\tau_n|} \hat{t}_n^{-1} \sigma_y$  and of the product of  $\begin{pmatrix} \mu_n / \sqrt{|\tau_n|} & 1 / \sqrt{|\tau_n|} \\ \text{sign}(\tau_n) \sqrt{|\tau_n|} & 0 \end{pmatrix}$ . The former product is very similar to the product  $\Pi_k \hat{t}_{2k}^{-1} \hat{t}_{2k-1}^\dagger$  studied earlier (note, however, the particular “normalization” used here); the Lyapunov spectrum consists of two exponents  $\pm \gamma_t$ , with  $\gamma_t$  of order one. The latter product is essentially the transfer matrix product at  $\epsilon = 0$  for a  $1d$  Anderson problem with random energies  $\pm \mu_n$  (depending on the sign of  $\tau_n$ ) and random hopping amplitudes  $\sqrt{|\tau_n|}$ ; the two corresponding exponents are  $\pm \gamma_\mu$ . The full Lyapunov spectrum thus consists of the four exponents  $\pm \gamma_t \pm \gamma_\mu$ . As we increase the strength of the rung couplings  $\mu_n$  (e.g., by increasing the root mean square strength  $R \equiv R_\mu \equiv \sqrt{\overline{\mu^2}}$  with  $\overline{\mu} = 0$  kept fixed) from 0 to  $\infty$ ,  $\gamma_\mu$  also increases from 0 to  $\infty$ . Thus, at some critical strength  $R = R_c$  of the rung couplings,  $\gamma_\mu$  will equal  $\gamma_t$ , and two Lyapunov exponents will be zero corresponding to an isolated delocalized critical point along the  $R$  axis.

Now, in the superconductor problem, there are no eigenstates at precisely zero energy in any system—this is due to the presence of the rung couplings. Nevertheless, there may be states with exponentially small (in system size) energy, and the localized phases on either side of the critical point can again be characterized in terms of such almost-zero-energy end-states. Consider again an open odd-length chain. When  $\mu_n \equiv 0$  (and  $\delta \equiv 0$ ), there are two zero-energy states, one at each end of the chain. Turning on the rung couplings enables the two to mix, but since they are separated by the entire length of the chain, the splitting is exponentially small in the length of the chain—as long as  $R < R_c$ . Thus, in this phase, there will be two such (essentially) zero-energy end-states. In terms of the quasiparticle spectrum of the original superconductor  $\hat{H}_{SC}$ , there is a *single* quasiparticle state with an exponentially small energy and a wavefunction with weight only at the two ends of the chain. On the other hand, in the phase with  $R > R_c$ , there are no such end-states with nearly zero energy, as may be argued by starting with the limit of large  $\mu_n$ . Thus, we have two different localized phases distinguished by this topological property; if we think in terms of a more general ‘dimerization’-‘rung coupling’ ( $\delta - R$ ) parameter plane, we have a phase diagram shown schematically in Fig 2. Moreover, we again expect the low-energy properties in the vicinity of the transition between the phases to be in the universality class of the single chain bipartite RH problem in the vicinity of its zero-dimerization critical point. In particular, we again expect Griffiths singularities in the density of states of either localized phase in the vicinity of the critical point—our expectations will

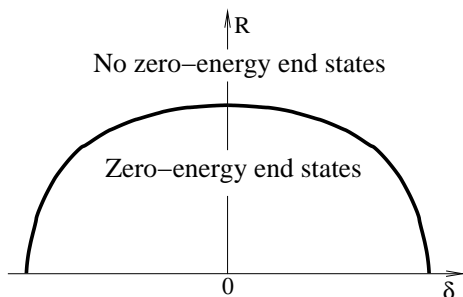


FIG. 2. Schematic phase diagram in the  $\delta - R$  plane for both the general spinless case without T-invariance, and the ‘spinful’ model with T-invariance. We use  $R$  to denote some measure of the strength of the rung couplings which correspond to the random on-site terms of the original superconductor problem (e.g., for a symmetric distribution of random rung couplings, we can define  $R$  to be a root mean square of this distribution). The vicinity of the phase boundary is expected to exhibit strong Griffiths effects.

be borne out by the more detailed RG analysis in the next section.

### 3. Single-channel spinful T-invariant superconductor:

Consider now the ‘spinful’ system with T-invariance (but no SR-invariance). In the bipartite representation, Eq. (6), the rung coupling is  $\hat{u}_n = \begin{pmatrix} 0 & w_n \sigma_y \\ w_n^* \sigma_y & 0 \end{pmatrix}$  with some c-number  $w_n$ , while the hopping term has a form  $\hat{t}_n = \begin{pmatrix} 0 & \hat{a}_n \\ \hat{b}_n & 0 \end{pmatrix}$  with  $\hat{b}_n = -\hat{a}_n^*$  but otherwise general complex  $2 \times 2$  matrix  $\hat{a}_n$ . From the transfer matrix, Eq. (9), the sublattice decoupling at zero energy is seen immediately; on one sublattice, we need only consider the product of

$$\hat{Q}_n = - \begin{pmatrix} \hat{a}_n^{-1} w_n \sigma_y & \hat{a}_n^{-1} \\ \hat{a}_n^T & 0 \end{pmatrix}. \quad (12)$$

Lyapunov exponents of this product together with their negatives (from the other sublattice) form the full Lyapunov spectrum of the system. But this product further “decouples” precisely as in Eq. (11) into the product of  $\sqrt{|\alpha_n|} \hat{a}_n^{-1} \sigma_y$  and the product of  $\begin{pmatrix} w_n / \sqrt{|\alpha_n|} & 1 / \sqrt{|\alpha_n|} \\ \alpha_n / \sqrt{|\alpha_n|} & 0 \end{pmatrix}$ ; here  $\alpha_n = \det \hat{a}_n$ . Lyapunov exponents of the former product are  $\pm \gamma_a$  with some  $\gamma_a$  of order one. However, the 1d Anderson localization problem corresponding to the latter product is non-hermitian: while the hopping amplitudes can be chosen real and equal to  $\sqrt{|\alpha_n|}$ , the on-site energies  $|w_n| e^{i\psi_n}$  are complex, with the phases  $\psi_n$  having contributions from the phases of both  $w$  and  $\alpha$ . Nevertheless, the Lyapunov spectrum still consists of two exponents  $\pm \gamma_w$ . The spectrum of the product of the  $\hat{Q}_n$  is thus  $\pm \gamma_a \pm \gamma_w$ , and

the other sublattice merely duplicates this to make the full Lyapunov spectrum doubly degenerate. Now, all we need to know is that for small values of rung-couplings the corresponding  $\gamma_w$  is also small, while for large values of rung-couplings  $\gamma_w$  is large. Then, as in the spinless case, there is an isolated delocalized critical point along the  $R \equiv R_w \equiv \sqrt{w^2}$  axis for some critical strength  $R_c$  of the rung coupling terms (at which  $\gamma_w = \gamma_a$ ). Note that at this critical point, a total of four Lyapunov exponents will simultaneously cross zero; the corresponding two pairs of critical modes are related to each other by T-invariance. Again, the phase with  $R < R_c$  is characterized by the presence of end-states with exponentially small energies. The only difference from the spinless case is that there are now four of them—this corresponds, in terms of  $\hat{H}_{SC}$ , to two T-symmetry related quasiparticle states, each with an exponentially small energy and a wavefunction having weight only at the two ends of the chain. The phase with  $R > R_c$  again has no such nearly-zero-energy end-states. In the full  $\delta$ - $R$  plane, we thus have the schematic phase diagram shown in Fig 2. Again, the critical point and the phases in its vicinity are expected to look, at low energies, like those in the single chain RH problem, with an additional degeneracy introduced by T-invariance. A direct numerical check of the Dyson form for the critical density of states in this ‘spinful’ T-invariant case is shown in Fig. 3, while the RG results of the next section confirm the underlying physical picture in detail.

Parenthetically, we also note that these Lyapunov exponent crossing arguments imply that in all cases considered so far, the inverse of the smallest Lyapunov exponent diverges as  $|g - g_c|^{-1}$  where  $g$  is some tuning parameter that drives the system through the critical point at  $g_c$ . This implies that the exponent  $\nu$  for the typical localization length is  $\nu = 1$  at all these transitions.

### 4. Single-channel spinful superconductor without T-invariance:

Finally, we turn to the ‘spinful’ case with neither T-invariance nor SR-invariance (again, with only a single transverse channel). [Note that a quasi-1d spinless fermion superconductor with *two* transverse channels would also be modeled by the same BdG problem, with a somewhat different interpretation for the various couplings. Thus, analysis of this case is of value in demonstrating that our basic conclusions are not special to the single-channel case in any of the problems we consider.]

In this case, we have been unable to come up with any simple decoupling scheme that maps the corresponding transfer matrix to that of some problem with sublattice symmetry—the exact mapping we have used earlier is thus special to the two single-channel cases considered above. However, when the rung couplings are all zero, we do know that the corresponding bipartite four-leg ladder has five phases as we scan the dimerization parameter

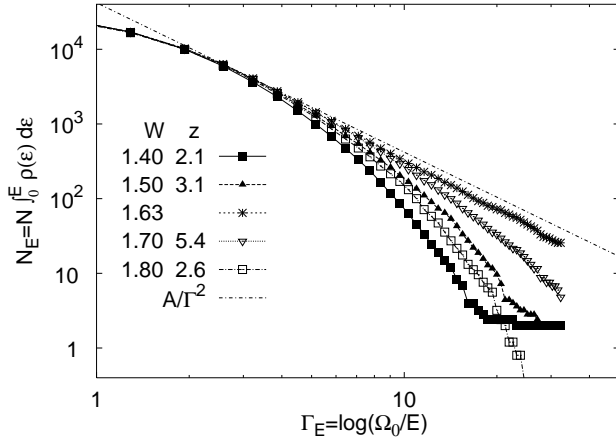


FIG. 3. Numerical check of the Dyson singularity in the ‘spinful’ T-invariant case. Number of states with energies between 0 and  $E$  for an open chain of length  $L = 10^5$ , averaged over 5 disorder realizations, is plotted vs the log-energy scale  $\Gamma_E = \ln(1/E)$ . Independent inter-site couplings (real and imaginary parts, of independent hopping and pairing amplitudes) are chosen from a uniform distribution over  $[-1, 1]$ , while independent on-site couplings (real chemical potential and real singlet pairing amplitude) are chosen from a uniform distribution over  $[-W, W]$ . Critical  $W_c = 1.630 \pm 0.001$  was found accurately from numerical transfer matrix analysis. At this point, we clearly have  $N_\Gamma \sim 1/\Gamma^2$  (which is shown displaced from the data for clarity). We also show several off-critical points and give rough estimates of the corresponding dynamical exponents  $z$  from the Griffiths fits  $N_E \sim E^{d/z}$  over  $4 < N_E < 1000$ .

$\delta$ —these are labeled  $(k, 4 - k)$  with  $k = 0, 1, 2, 3, 4$  corresponding to  $4 - k$  zero-energy states localized at one end and  $k$  states localized at the other end for a finite ladder with an odd number of rungs and free boundary conditions. In particular, in the vicinity of  $\delta = 0$  one has two such states at each end. Now, turning on some weak rung couplings allows these two states (at each end) to mix amongst themselves, and there will thus be no states with exponentially small energies in this regime. On the other hand, the same is clearly true for very large values of the rung couplings. Thus, the phases obtained in either case in the vicinity of  $\delta = 0$  are expected to ‘look’ the same (this is made more precise later using our RG approach).

The question then arises: Is there a single intervening phase (at  $\delta = 0$ ) which is topologically different? This would result in *two* phase transitions as we scan the magnitude of the rung couplings. Another simple possibility is that there is no transition at all as a function of increasing rung coupling. Of course, there can also be other more complicated scenarios (some possibilities for the full phase diagram are sketched in Fig. 4). Moreover, since there are several independent rung couplings corresponding to each physical lattice site, there are many different ways of ‘increasing the rung coupling’ and the possible

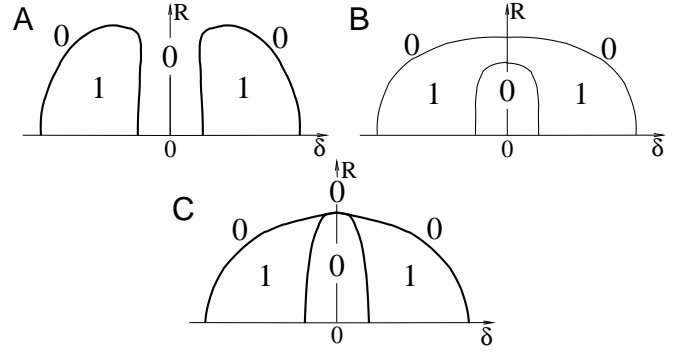


FIG. 4. Possible phase diagrams in the  $\delta - R$  plane for the ‘spinful’ case without T-symmetry. We use  $R$  to represent some measure of the strength of the rung-couplings. On the diagrams, we denote the phases with zero-energy end-states by 1 and the phases with no such states by 0. A and B represent two simple possibilities, while a more complicated case with a multi-critical point is shown in C. Our numerical transfer matrix studies tentatively suggest that in the most ‘random’ such superconductor (i.e., with all couplings present and independent) the phase diagram is very nearly that of the panel C. In many other cases (e.g., when we allow only on-site chemical potentials in the original superconductor problem, but completely general inter-site couplings), we observe the phase diagram A. We have not found realizations that would clearly exhibit the phase diagram B; however, we do not have arguments that would rule out this possibility.

phases and transitions encountered along the way will most likely depend on how we scan.

To get a more detailed picture, we performed an extensive numerical transfer matrix analysis (to obtain accurate results, we used the technique of Ref. 20), as well as exact diagonalization studies, for particular choices of scan. In one choice of scan, we include all possible inter-rung couplings, but allow only those (intra-)rung couplings that correspond to random on-site chemical potentials in the original superconductor problem. In this case, we can clearly delineate the phase boundaries to conclude that we have a phase diagram of the type shown in Fig. 4A, with no transition along the  $R$  axis at  $\delta = 0$  (with  $R$  now a measure of the strength of the on-site potentials). If we scan across the phase boundary at a fixed non-zero value of dimerization (so that we start in the phase with zero-energy end-states and leave it by increasing the mean-square strength of the random potentials), we find that the typical localization length defined by the inverse Lyapunov exponent again diverges with an exponent  $\nu = 1$ , and the critical density of states is again of the Dyson form.

In another scan, we take the most random such system (i.e., with all allowed couplings present and independent) and boost the strength of all the (independent) rung couplings by the same amount on average, while keeping distribution of the inter-rung couplings fixed. As we increase the typical magnitudes of the rung couplings from



zero in this manner, we again see strong Griffiths singularities in the density of states developing, and, possibly, critical behavior. However, near such a tentative critical point the two Lyapunov exponents that come close to zero seem to have a mutual “level repulsion” and the Lyapunov spectrum seems to exhibit the analog of an “avoided level crossing”; this results in huge localization lengths and strong near-critical behavior in large regions around the tentative critical point. A more detailed investigation away from  $\delta = 0$  yields a phase diagram of the type shown in Fig. 4C. Thus, to within our numerical accuracy, there seems to be a multicritical point in the  $\delta - R$  phase diagram at  $\delta = 0$ . However, we can not exclude the possibility that we are seeing a case with no transition along the  $R$ -axis (but phase-boundaries coming very close to this axis) or an almost-degenerate case with two very closely spaced transitions. Crossing the phase boundaries away from the putative multi-critical point again gives a localization length exponent of  $\nu = 1$ . However, we are unable to make any reliable statements in the vicinity of the multicritical point.

We have scanned along several other directions in the parameter space (corresponding to different interpretations of the rung-coupling parameter  $R$ ), but have not clearly seen two distinct transitions as in Fig. 4B; however, behavior of the type shown in Fig. 4A is the most common. [However, note that the weak-disorder analysis of Ref. 5 did find critical behavior in the conductance at  $\delta = 0$  with inter-rung and intra-rung couplings identically distributed and chosen from a Gaussian distribution. Moreover, their result is consistent with our predictions for critical behaviour at ‘ordinary’ critical points, as opposed to multicritical points.]

These numerical results thus confirm our suspicion that the structure of the full phase diagram in this general ‘spinful’ case (or in multi-channel versions of all the cases) is quite complicated. The specific phase diagram obtained by tuning the parameters of a particular physical system (in which some subset of the allowed couplings may be identically zero) can thus be very different from case to case (a similar observation in related  $2d$  models has been made in Refs. 20 and 21). However, it is clear that there can be, in general, two kinds of localized phases. Moreover, whenever both phases are present in the phase diagram of a particular system, we again expect (analogous to the single-channel cases considered above) the system in the vicinity of the phase boundary to ‘look’ at low-energies like a single-chain random hopping problem with weak dimerization (note that the numerical estimate,  $\nu = 1$ , that we obtain away from any special ‘multicritical’ points supports this picture, and our RG results provide further confirmation of the same).

This is as far as we can go with an elementary transfer matrix analysis. For a more detailed characterization of the low-energy properties, we now turn to the strong disorder RG analysis.

## VI. CRITICAL POINTS AND GRIFFITHS EFFECTS IN 1D: RG ANALYSIS

To test the above picture in detail, we have implemented the RG numerically in all three single-channel cases. Since the single-channel spinful problem without T-invariance is essentially identical to the corresponding two-channel spinless problem, this last example also serves to establish that our conclusions do not depend on any special properties of the single-channel case. In the single-channel spinless case without T-symmetry (and the corresponding spinful case with T-invariance), we focus mainly on the vicinity of the phase transition at  $\delta = 0$  (see Fig. 2). In the ‘spinful’ case without T-invariance, we consider the two different realizations described in the previous section—these have phase diagrams of the types shown in Fig. 4A (in which we scan across the phase boundary at non-zero dimerization so that we leave the phase having end-states by increasing the strength of the onsite potentials) and in Fig. 4C (in this case, we focus on the immediate vicinity of the putative multicritical point). [For completeness, we have also studied the transitions as a function of dimerization in the bipartite ladder problems of Sec. V 1.]

For the  $\delta = 0$  spinless case, (and the ‘spinful’ T-invariant case) we consider systems with lengths as large as  $L = 2 \times 10^5$ . The initial conditions used have random (inter-rung) hoppings chosen from a uniform distribution over  $[-1, 1]$ , and random (intra-rung) couplings  $u$  chosen from a symmetric (with either sign equally probable) power law distribution  $P(u) = \frac{1}{2g}|u|^{-1+1/g}$ ,  $|u| \leq 1$ . Note that the RG transformation (7) can be formulated entirely in terms of the imaginary parts of the couplings, and this is the language that we use here. For the ‘spinful’ case without T-symmetry, we are restricted to  $L \leq 5 \times 10^4$ . When we scan at finite dimerization, we enforce this dimerization by choosing the even and odd inter-rung couplings from the power law distribution  $P(u)$ , but with different fixed values  $g_{\text{even}} \neq g_{\text{odd}}$  for the power law exponents. The strength of the rung couplings is again tuned by varying the corresponding power-law exponent  $g_{\text{rung}}$ . We use the “full” RG rule (7) rather than its less accurate “max” version since we are primarily interested in testing our physical picture for the low-energy properties starting with a system with moderate values of the bare disorder.

Apart from the immediate vicinity of the putative multicritical point of Fig. 4C (which we comment upon separately), our results are equally reliable and essentially identical in all the cases studied. In the interests of brevity, below we display in detail only the results obtained in the spinless case at  $\delta = 0$  (see Fig. 2).

We search for the critical point by looking at the fraction of “isolated” sites among the remaining sites in the system: If there are  $N$  sites left, we find all the sites that are “covered” by the  $N/2$  strongest remaining bonds. Roughly speaking, the fate of these covered sites

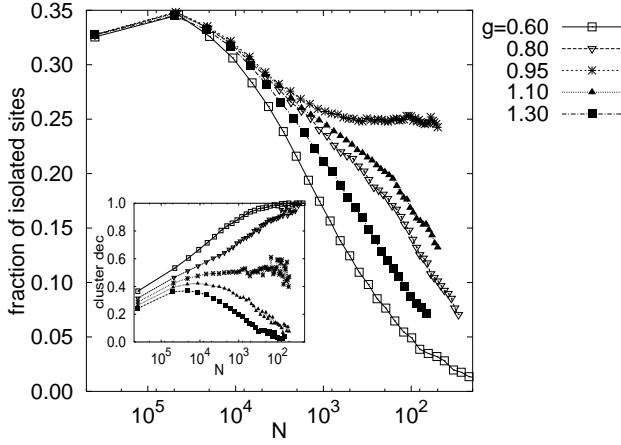


FIG. 5. Fraction of isolated sites among the remaining sites for the two-leg ImRH ladder representing spinless fermion superconducting wire. Critical  $g_c \approx 0.95$  is clearly identified. Inset shows the fraction of cluster decimations (see text for details).

is clear—they will be frozen dynamically at roughly this log-energy scale. The rest of the sites are still dynamically free at this scale, and we call them “isolated”. In a localized phase, this fraction quickly approaches zero. On the other hand, at a critical point, we expect that new couplings which contribute, upon their subsequent decimation at a lower energy, to the density of states at that lower scale, are formed continually over all energy scales in a scale-invariant way. The fraction of isolated sites at criticality is therefore expected to saturate to some constant at low energies. In the case of a single critical RH chain, a quarter of the remaining sites is notionally isolated at each stage of the RG: each site has a bond to the right and to the left, and the bond strengths are uncorrelated; since each bond has a 50% chance of being “weak”, the site is “isolated” with probability  $1/4$ . This gives us a very direct test for the location and nature of the critical point.

Results of such a search for our spinless case are shown on Fig. 5. We clearly identify a critical  $g_c \approx 0.95$ , and note that the fraction of isolated sites at this critical point remains essentially 0.25, which is evidence that the low-energy behavior is that of a single one-dimensional ‘backbone’ that goes critical. Note that it is also possible to further probe the geometry associated with the low-energy theory, as is done, e.g., below in our “order-parameter” studies, and even more exhaustively by looking in detail at probability distributions of the various couplings (which we have not pursued fully—the RG results shown here already confirm our basic picture of the low-energy physics).

At the critical point, the number of sites remaining at the log-energy scale  $\Gamma \equiv \ln(\Omega_0/\Omega)$  is  $N_\Gamma \sim 1/\Gamma^2$ , as can be readily seen from Fig. 6. Since  $N_\Gamma$  is essentially the integrated density of states, this is consistent with the

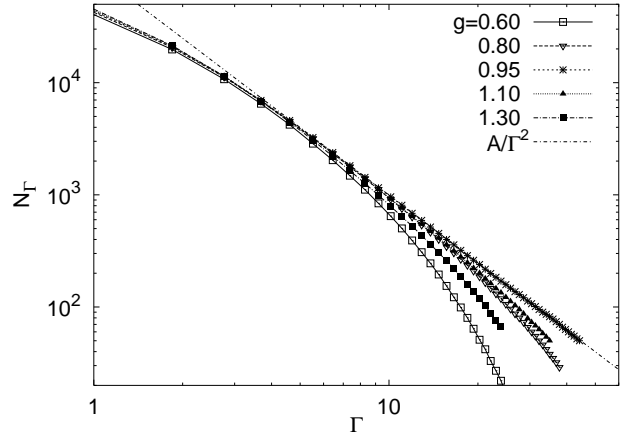


FIG. 6. Number of remaining sites  $N$  vs log-energy scale  $\Gamma$ . Also shown is the fit of the critical  $N_\Gamma$  to the form  $A/\Gamma^2$ .

Dyson  $\rho(\epsilon) \sim 1/|\epsilon| \ln^3 |\epsilon|$ . Moreover, at  $g = g_c$ , the distributions of all couplings become broader and broader on the *logarithmic* scale, with the characteristic widths growing linearly with  $\Gamma$ . This is shown on Fig. 7. In conjunction with our result for the fraction of isolated sites at low energies at criticality, this indicates that the critical point is in the same universality class as the single chain RH problem. [Note that since the system effectively reduces to a single RH chain ‘back-bone’ in the low-energy limit, we expect<sup>19</sup> the critical average thermal conductance  $\kappa_c(L)$  of the original superconductor to scale as  $k_B T/\sqrt{L}$ , where  $L$  is the length of the wire—this is consistent with the weak disorder result of Ref. 5. As mentioned earlier, this leads us to believe that their analysis was performed only at such a critical point and does not represent the generic behavior of the system.]

Consider now the two different localized Griffiths phases. As expected, we find  $N_\Gamma \sim e^{-\Gamma/z}$  with a continuously varying dynamical exponent  $z$  which diverges as  $z \sim |g - g_c|^{-1}$  (to within our numerical accuracy) as we tune across the critical point. Within our strong-disorder approach, the two Griffiths phases are distinguished by the character of the corresponding RG-generated dimer patterns. To discuss this intuitive distinction more precisely, we compare such RG-generated dimer covers against some fixed *reference dimer cover*. A natural choice of the reference cover for the spinless problem at hand is a “vertical” cover with reference dimers covering the rungs of the ladder, i.e., joining the two copies of each of the original fermions of  $\hat{H}_{SC}$ . We use this specific reference cover in our numerical studies presented below; the following discussion, however, is fairly general. [We use the same ‘vertical’ reference cover in the other two superconductor problems we study with the RG.]

We call two sites connected by such a reference bond a *cluster*, and the corresponding coupling between the two sites a *field* on the cluster. Couplings that connect sites in

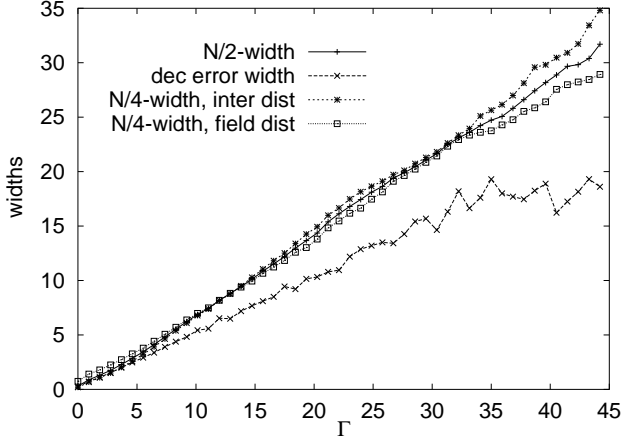


FIG. 7. At the critical point (determined from Fig. 5) different measures of the widths of the *log*-coupling distributions all scale linearly with  $\Gamma$ . We plotted the  $N/2$ -width of the distribution of all bonds, the ‘decimation error’ width (defined as the average logarithm of the ratio of the decimated bond to the strongest nearby bond), and also the  $N/4$ -widths of the interaction and field distributions with respect to the vertical reference cover (see text for details).

different clusters are called *interactions* between the clusters. This terminology is borrowed from the 1d random transverse field Ising model (RTFIM), but we emphasize that the correspondence is *not* exact although we do expect that the *critical* behavior, characterized with respect to a well-chosen cover, is essentially that of the RTFIM (we expect this to be true because a similar analysis for the dimerized single chain random hopping problem using the natural reference cover consisting of alternate bonds gives an exact mapping to the 1d RTFIM). When a coupling connecting two sites in the same cluster is decimated (field decimation), the corresponding cluster is *killed*. When a coupling connecting two sites in different clusters is decimated (interaction decimation), the two clusters are *joined* into one new cluster, which is now specified by the two other (remaining) end-points of the two original clusters. The number of original sites that belong to a cluster defines its ‘magnetic moment’ and it then makes sense to talk of a magnetization density  $m$  for the system. Pictorially, a reference dimer cover specifies some connectivity rules for the RG-formed dimers, with natural notions of clusters and percolation with respect to such connectivity rules, while the RG rules prescribe the dynamics (as a function of increasing  $\Gamma$ ) obeyed by the clusters. Such connectivity properties can be used to distinguish between different RG-generated dimer covers, and, thus, to characterize the different phases.<sup>22</sup> Within the strong-disorder RG, this is the distinction that captures the different ‘topological’ character of the two Griffiths phases.

Going back to our numerical RG studies, we find that, with respect to the vertical reference cover, in the phase

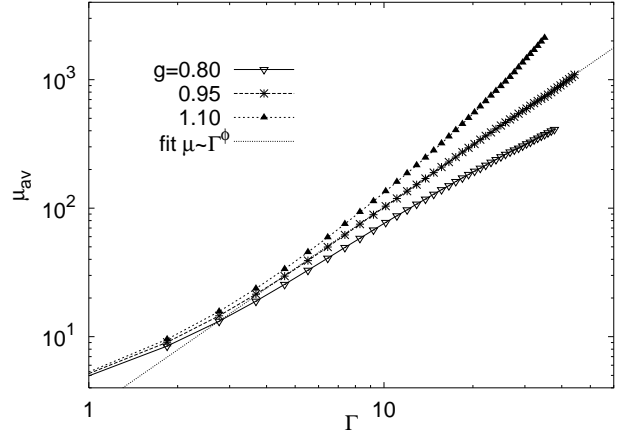


FIG. 8. Average moment of the remaining clusters with respect to the vertical reference cover. Also shown is the fit at the critical point for the exponent  $\phi$ . From this fit we obtain  $\phi \approx 1.59$ , which can be compared with the corresponding exponent for the quantum Ising model,  $\phi_{\text{RTFIM}} = (1 + \sqrt{5})/2 \approx 1.62$ .

which obtains for strong rung couplings (small values of  $g$ ) there are only small clusters and no connectedness across the whole system, while for weak rung couplings (large values of  $g$ ) there is an infinite percolating cluster that forms in the limit of large  $\Gamma$ . This development of topological order for  $g > g_c$  is characterized by an exponent  $\beta$  defined by the scaling of the average magnetization density:  $m(\Gamma \rightarrow \infty) \sim (g - g_c)^\beta$ . At criticality, the average moment of the surviving clusters scales as  $\mu \sim \Gamma^\phi$ , which defines the exponent  $\phi$ ; in complete analogy to the RTFIM,<sup>23</sup> the exponent  $\beta$  for the topological order parameter (‘magnetization’) can be obtained from  $\phi$  via the scaling relation  $\beta = 2 - \phi$ . Figure 8 shows our numerical result for the  $\Gamma$  dependence of the average moment of the surviving clusters at the critical point. The numerical value obtained for the exponent  $\phi$  is very close to that of the 1d RTFIM. The value  $\beta \approx 0.41$  we infer using the scaling relation is then very close to the corresponding exact result for the single dimerized chain (which has a  $\beta$  exactly equal<sup>24</sup> to the magnetization exponent  $(3 - \sqrt{5})/2$  of the 1d RTFIM<sup>23</sup>). We also note that, similarly to the quantum Ising model, the critical point is the point of balance between the cluster fields and cluster interactions; this is shown in the inset of Fig. 5, and provides alternative means for identifying the critical point. This completes our RG description of the spinless case.

Essentially the same results are obtained for the corresponding spinful problem with T-symmetry—this is consistent with our general argument in Section IV. We also repeated this analysis for the specific realization of the spinful problem without T-symmetry corresponding to Fig. 4A. All the results obtained for this case in the vicinity of the transition at fixed finite dimerization (as a function of increasing  $R$ ) are essentially identical to the

results shown above for the spinless case. [Entirely analogous results are also obtained in all cases for the dimerization driven transitions of the bipartite ladder problems.] Thus, our general picture for the low-energy physics appears to be validated by the RG results so long as we are not in the vicinity of any special multicritical points.

Finally, a brief comment on the RG results in the vicinity of the putative multicritical point, Fig. 4C. As we scan R at  $\delta = 0$ , strong Griffiths effects again show up clearly over a wide region in the vicinity of the putative multicritical point. Moreover, the phases at large and small R both look ‘paramagnetic’ in terms of clusters defined with respect to the vertical reference cover (and also many other reference covers). This is consistent with our arguments in the previous section. However, our RG results are also inconclusive when it comes to pinning down the structure of the phase diagram near this apparent multicritical point—again the analysis is plagued by near-critical behavior over a wide region. The corresponding long crossovers do not allow us to make any definitive statements regarding either the presence or the universality class of such multicritical points. This remains the principal unresolved question in our entire analysis of the one dimensional examples.

## VII. HOW ARE THE LOW-ENERGY STATES GENERATED?

We now consider precisely how the states in the singular low-energy tail of the density of states are generated, and identify the corresponding Griffiths regions in the ImRH language. As is already implicit in the above discussion, such a pair of low-energy states is formed if there are two ‘isolated’ sites separated by a region in which all the other sites are locked into short-ranged (dimer) pairs. Griffiths effects are a consequence of such isolated sites being generated sufficiently often. An example of a pair of such sites is shown in Fig. 9. The isolated sites are very weakly coupled to each other—the coupling is of order  $\epsilon \sim e^{-cl}$ , where  $l$  is the length of the region. In a disordered system, there is always a probability of order  $p^l$ , with some  $p < 1$ , of finding such a region—this gives a power-law contribution  $\sim \epsilon^{|\ln p|/c}$  to the integrated density of states from such regions. Thus, we *always* expect a variable power-law (Griffiths) density of states in such random hopping problems in which *no on-site energies* (i.e., diagonal terms) are allowed; we conclude that Griffiths phases are *generic*. The specific example shown in the figure is expected to be relevant to Griffiths effects in the phase in which the rung couplings dominate on average. The regions to the left and to the right of the pair are intended to be a caricature of the *typical* regions in this regime, while the region in the middle is comparatively *rare*. Decreasing the strength of the rung couplings would increase the probability of having such regions, corresponding to the observed increase in the dynamical exponent as one approaches the transition to

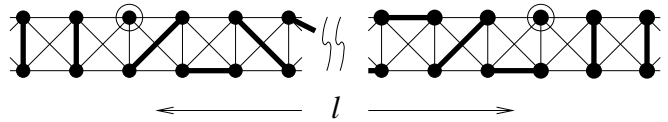


FIG. 9. Griffiths generation of low-energy states.

the other phase. The critical point is then characterized by a proliferation of such Griffiths regions on all energy scales.

The picture that emerges is thus very similar to that in our toy-model of Sec. II in which the low-energy states are closely associated with ‘domain walls’ between the two different gapped phases of the pure system.

It is useful, at this point, to recast some of this in terms of the original superconductor Hamiltonian  $\hat{H}_{SC}$ . This will give us a somewhat different perspective on the origin of these low-energy states. For simplicity, we restrict the discussion below to the spinless case. We first examine the basic RG rule Eq. (7). Consider a two-site problem

$$\hat{H}[\alpha, \beta] = \epsilon_\alpha c_\alpha^\dagger c_\alpha + \epsilon_\beta c_\beta^\dagger c_\beta + (t c_\alpha^\dagger c_\beta + \Delta c_\alpha^\dagger c_\beta^\dagger + \text{h.c.}).$$

This can be diagonalized by an appropriate Bogoliubov transformation to give<sup>25</sup>

$$\begin{aligned} \hat{H}[\alpha, \beta] &= \epsilon_+ \gamma_+^\dagger \gamma_+ + \epsilon_- \gamma_-^\dagger \gamma_- + \text{const}, \\ \epsilon_\pm &= \frac{1}{2} \left| \sqrt{(\epsilon_\alpha + \epsilon_\beta)^2 + 4|\Delta|^2} \pm \sqrt{(\epsilon_\alpha - \epsilon_\beta)^2 + 4|t|^2} \right|. \end{aligned}$$

From this solution, it is clear that states at both  $\alpha$  and  $\beta$  simultaneously contribute to either eigenstate only if either  $|t| \gtrsim |\epsilon_\alpha - \epsilon_\beta|$  or  $|\Delta| \gtrsim |\epsilon_\alpha + \epsilon_\beta|$ . When this happens, we can no longer think of the two sites in isolation and need to account for the *resonance* between them. Now, if  $|t|^2 - |\Delta|^2 \sim \epsilon_\alpha \epsilon_\beta$ ,  $\epsilon_-$  for such a resonance can be very small. In order to obtain a good low-energy description in such a situation, we would eliminate the high energy ‘+’ state and keep only the ‘−’ state by introducing a single *effective* site with site energy  $\epsilon_-$ . In our ImRH RG language, this corresponds to a situation in which a single bond connecting sites on two different rungs is decimated, leaving behind one site on each rung; these two remaining sites are coupled by a weak bond precisely equal in magnitude to  $\epsilon_-$ . On the other hand, if there is no mixing of the states at  $\alpha$  and  $\beta$ , i.e., when one of the local potentials, say  $\epsilon_\alpha$ , dominates, we would eliminate the state  $\alpha$  completely; in the ImRH RG this corresponds to decimating the corresponding rung. Thus, our RG procedure either eliminates a full fermion state because it is frozen out by a strong local potential, or eliminates ‘half of a fermion’ from each of the two sites in resonance and recombines the remaining halves to create a new effective fermion with site energy equal to the new coupling introduced (our RG is thus really defined on the corresponding Majorana fermion states).

Now, consider for concreteness the Griffiths phase in which the on-site potentials dominate. At low enough

energies, a description in terms of isolated effective sites (with negligible mixing between them) with some renormalized distribution of effective site energies is clearly appropriate. However, to arrive at such a description, one has to first account for all the resonances at higher energy scales that arise from any anomalous regions in which hopping and pairing amplitudes are large compared to local potentials. As a specific example of such anomalies, consider the central region of Fig. 9. In the original superconductor language, this region corresponds to both  $\Delta$  and  $t$  being relatively large and comparable in magnitude, in addition to having a somewhat definite relationship between their phases throughout this region. Eliminating all the resonances between the sites in this region finally gives a low-energy description in terms of a single effective site with an exponentially small energy. This effective site in the original superconductor language clearly corresponds, in the ImRH language, to the pair of isolated sites shown in Fig. 9. The ImRH RG thus provides the natural language for capturing the important low-energy physics. Crudely speaking, the ‘effective site-energies’ in the original superconductor language correspond to the ‘cluster field couplings’ with respect to the natural vertical reference dimer cover in the ImRH RG language. Note also that an important ingredient of the physical picture that emerges is the spatial character of the quasiparticle states (in particular, note that wavefunction of a low-energy quasiparticle in the phase with zero-energy end-states is split into two spatially separated pieces). Such spatial information is also kept most naturally in the ImRH RG; in particular, the development of the ‘topological order’ is seen most naturally in this language.

Finally, we can now go back and ask what is the precise role played by the various symmetry restrictions. As discussed above, Griffiths effects in the ImRH RG language are associated with situations in which we repeatedly eliminate only a subset of the couplings connecting two rungs (for instance, only *one* of the couplings in the spinless example above), thus splitting the original fermion states. Now, if some symmetry restrictions require that some of the original couplings between rungs equal one another, then we would be forced to decimate several of them simultaneously—for example, we could be forced to eliminate only complete fermion states. Within the RG approach, this could then rule out the possibility of Griffiths effects. It is easy to see that the restrictions imposed by T-invariance are not enough for this to happen. On the other hand, *in the SR-invariant case*, a simple analysis of the symmetry constraints for the corresponding ImRH problem shows that this is precisely what happens.<sup>26</sup> In the strong disorder limit, this, then, is the true significance of the absence or presence of SR-invariance for quasiparticles of a superconductor.

## VIII. DISCUSSION

In this article, we have established the existence of strong Griffiths effects in one-dimensional superconducting wires in which the quasiparticle spin is not a good quantum number. We associated these singularities with quasiparticle states that live on ‘domain walls’ between adjacent large regions in two different phases, one phase that supports zero modes localized near the ends of a finite system, and another that does not support such modes.

An obvious question now arises: Do such effects exist in two or more dimensions? Thinking in terms of the ImRH RG, it does seem that such effects could exist in cases without SR-invariance, particularly in the vicinity of the thermal-metal to thermal-insulator transition, or the transition between the two topologically distinct insulating phases in cases without T-symmetry. However, it is of course not *a priori* clear if ‘isolated sites’ would be produced sufficiently often in the RG for this to happen. Moreover, the extent to which such isolated sites can be associated, as in one dimension, with domain walls between topologically distinct regions is also not clear. Another obvious question is whether any of the phase transitions mentioned above are controlled by infinite-disorder fixed points. Although we have not studied all these questions carefully, it is clear that our strong-disorder RG approach, implemented numerically, provides the natural tool for such investigations in more than one dimensions. [So far, we have extensively studied only a related  $2d$  bipartite random hopping problem<sup>15</sup> using a similar RG approach<sup>18</sup> and found that such Griffiths effects do occur in this case: When we introduce enforced dimerization into this random hopping problem, we observe a transition between different Griffiths phases and tentatively conclude that the critical point is controlled by an infinite-randomness fixed point. Details of this study will be reported elsewhere<sup>16</sup> and could be relevant for certain models for spinless T-invariant  $2d$  superconductors in the presence of disorder.]

## IX. ACKNOWLEDGEMENTS

We would like to thank F. D. M. Haldane, B. I. Halperin, M. Hastings, I. Gruzberg, R. Moessner, and A. Vishwanath for valuable discussions, and C. Mudry and T. Senthil for useful comments on the manuscript. One of us (KD) was supported by NSF grant DMR-9809483 while at Princeton and is currently supported by NSF grant DMR-9981283 at Harvard. The others acknowledge support of NSF grant DMR-9802468.

- <sup>1</sup> T. Senthil *et al.*, Phys. Rev. Lett. **81**, 4704 (1998); T. Senthil and M. P. A. Fisher, Phys. Rev. B **60**, 6893 (1999); S. Vishveshwara, T. Senthil, and M. P. A. Fisher, *ibid.* **61**, 6966 (2000); R. Bundschuh *et al.*, *ibid.* **59**, 4382 (1999); R. Bundschuh *et al.*, Nucl. Phys. B **532**, 689 (1998).
- <sup>2</sup> T. Senthil and M. P. A. Fisher, Phys. Rev. B **61**, 9690 (2000).
- <sup>3</sup> See however, C. Pepin and P. A. Lee, cond-mat/0002227; W. A. Atkinson *et al.*, Phys. Rev. Lett. **85**, 3926 (2000).
- <sup>4</sup> F. J. Dyson, Phys. Rev. **92**, 1331 (1953).
- <sup>5</sup> P. W. Brouwer, A. Furusaki, I. A. Gruzberg, and C. Mudry, Phys. Rev. Lett. **85**, 1064 (2000).
- <sup>6</sup> M. Titov, P. W. Brouwer, A. Furusaki, and C. Mudry, cond-mat/0011146.
- <sup>7</sup> After this paper was completed, we learned that the generic localized behavior predicted by us can also be studied using the supersymmetry method for the special case of a 1d single-channel spinless superconductor without T-invariance (I. Gruzberg *et al.*, private communication).
- <sup>8</sup> N. Read and D. Green, Phys. Rev. B **61**, 246 (2000).
- <sup>9</sup> This distinction between the two phases of the pure system can also be stated in topological terms as in Ref. 8.
- <sup>10</sup> For examples of such self-consistent calculations, see A. Ghosal, M. Randeria, and N. Trivedi, cond-mat/0004481, Phys. Rev. Lett. **81**, 3940 (1998); see also K. Sengupta *et al.*, cond-mat/0010206 for a one-dimensional self-consistent calculation closely related to our toy model.
- <sup>11</sup> A. A. Abrikosov, J. Low Temp. Phys. **53**, 359 (1983).
- <sup>12</sup> H. J. Schulz and C. Bourbonnais, Phys. Rev. B **27**, 5856 (1983).
- <sup>13</sup> A. Altland and M. R. Zirnbauer, Phys. Rev. B **55**, 1142 (1997).
- <sup>14</sup> P. W. Brouwer, C. Mudry, and A. Furusaki, Phys. Rev. Lett. **84**, 2913 (2000); P. W. Brouwer, C. Mudry, B. D. Simons, and A. Altland, *ibid.* **81**, 862 (1998).
- <sup>15</sup> R. Gade, Nucl. Phys. B **398**, 499 (1993); R. Gade and F. Wegner, *ibid.* **360**, 213 (1991).
- <sup>16</sup> O. Motrunich, K. Damle, and D. A. Huse, *in preparation*.
- <sup>17</sup> O. Motrunich, K. Damle, and D. A. Huse, cond-mat/0005543.
- <sup>18</sup> Note that this is a natural generalization of the RG transformation  $\tilde{t}_{iA,jB} = t_{iA,jB} - t_{iA,2B}(t_{2B,1A}^*)^{-1}t_{1A,jB}$  introduced in previous work<sup>17</sup> to treat a bipartite random hopping problem (in which sites of the ‘A’ sublattice are only coupled to those of the ‘B’ sublattice). In this case too, no diagonal terms are generated and the problem remains bipartite. However, for a general hopping problem (not pure imaginary) on a non-bipartite lattice the transformation Eq. (7) generates diagonal terms (corresponding to random site energies), and the system is in the usual universality class of Anderson localization.
- <sup>19</sup> L. Balents and M. P. A. Fisher, Phys. Rev. B **56**, 12970 (1997); H. Mathur, *ibid.* **56**, 15794 (1997).
- <sup>20</sup> J. T. Chalker *et al.*, cond-mat/0009463.
- <sup>21</sup> N. Read and A. W. W. Ludwig, cond-mat/0007255.
- <sup>22</sup> Connectivity with respect to a given cover measures the following *string correlator*

$$C(i, j) = \frac{\langle G | (2\hat{n}_i - 1)(2\hat{n}_j - 1) \Pi_{p \in \text{ref}} (f_{p,1}^\dagger f_{p,2} - f_{p,2}^\dagger f_{p,1}) | G \rangle}{\langle G | \Pi_{p \in \text{ref}} (f_{p,1}^\dagger f_{p,2} - f_{p,2}^\dagger f_{p,1}) | G \rangle},$$

where  $\Pi_{p \in \text{ref}}$  denotes the product over *all* dimers  $p$  of the reference cover, and  $|G\rangle$  is the ground-state Slater determinant obtained from the strong-disorder RG. One can easily show that  $C(i, j) = 1$  if and only if the two sites belong to the same cluster, and  $C(i, j) = 0$  otherwise. A similar “cluster description” for a topological order parameter was used in the study of random antiferromagnetic spin-1 chains in C. Monthus, O. Golinelli, and Th. Jolicoeur, Phys. Rev. Lett. **79**, 3254 (1997).

- <sup>23</sup> D.S. Fisher, Phys. Rev. B **51**, 6411 (1995).
- <sup>24</sup> Note that the value of the exponent  $\beta$  for the string order parameter of a single dimerized chain used by us here for the purposes of comparison is different from the (incorrect) value quoted in R. A. Hyman, K. Yang, R. N. Bhatt, and S. M. Girvin, Phys. Rev. Lett. **76**, 839 (1996).
- <sup>25</sup> L. S. Levitov, Ann. Phys. (Berlin) **8**, 697 (1999).
- <sup>26</sup> The same is true if we write the usual Anderson localization problem in the ImRH language—this is consistent with the expectation that disorder does not lead to any singular behavior of the density of states at the Fermi energy in a normal, non-interacting electron system.